High-capacity amidoxime functionalized β-cyclodextrin/graphene aerogel for selective uranium capture

Nan Li,[a] Li Yang,[b,c] Dong Wang,[a] Chuyang Tang,[d] Weiqiao Deng,[b,c] Zhining Wang[a,]*

a. Shandong Provincial Key Laboratory of Water Pollution Control and Resource Reuse, School of Environmental Science and Engineering, Shandong University, Qingdao 266237, P. R. China

b. Institute of Molecular Sciences and Engineering, Institute of Frontier and Interdisciplinary Science, Shandong University, Qingdao 266237, P. R. China

c. State Key Laboratory of Molecular Reaction Dynamics, Dalian National Laboratory for Clean Energy, Dalian Institute of Chemical Physics, Chinese Academy of Sciences, Dalian 116023, P. R. China

d. Department of Civil Engineering, The University of Hong Kong, Pokfulam, Hong Kong 999077, P. R. China

KEYWORDS: graphene aerogel; β-cyclodextrin; amidoxime; uranium extraction; oil pollution resistance

ABSTRACT: Uranium extraction from seawater is a grand challenge of mounting severity as the energy demand increases with a growing of global population. An amidoxime functionalized β-cyclodextrin/graphene aerogel (GDC) is developed for highly efficient and selective uranium extraction via a facile one-pot hydrothermal process. The abundant functional uranyl-binding sites on GDC provided by amidoxime and other oxygen groups exhibit a uranium adsorption capacity of 654.2 mg/g with a short saturation time of 1 hour. Benefited from the chelation and complexation reaction, the obtained GDC achieves an excellent selectivity even when the competitive cations, anions and oil pollution exist. In addition, the aerogel possesses excellent mechanical integrity and remains intact after ten compression cycles. Meanwhile, the GDC can be easily regenerated and remains a high reusability of 87.3% after ten adsorption-desorption cycles. It is worthwhile mentioning that GDC performs an excellent extraction capacity of 19.7 mg/g within 21 days in natural seawater, which is greatly desired in uranium extraction from seawater.

INTRODUCTION

Augmenting energy supply by nuclear power is crucial for alleviating global energy crisis.[1] Uranium, as the vital source material for nuclear energy, will be in great demand with the rapid development of nuclear industry.[2] However, the land deposits of uranium

minerals are limited and forecasted to be exhausted in this century from worldwide consumption.[3] Therefore, the selective extraction of uranium from seawater is of great significance, because the oceans reserve enormous uranium, which is thousands times more than the terrestrial resources.[4] Great efforts have been made to develop efficacious uranium separation and recovery systems for addressing the challenges including the ultralow uranium concentration (~3.3 μg/L), various competitive ions and complex environments in seawater.[5]

Uranium extraction by adsorption technology exhibits the highest feasibility, due to its high cost-efficiency.[6] The unique demands of uranium extraction from seawater engender ideal adsorbents with the features of high specific surface areas, abundant selective binding sites as well as rapid mass transfer properties. Through control over material chemical property, morphology and structure, novel adsorbents offer high sorption capacity, prominent selectivity, fast removal kinetics, excellent reusability and exceptional fouling resistance. High-performance adsorbents can not only improve the efficiency and flexibility of uranium recovery from seawater, but also mitigate the long-term extraction cost.

Large surface area plays a critical role to increase the adsorption capacity and accelerate the kinetics by providing more adsorption sites. The engineered architectures of sorbents, such as sponge structure, microporous membrane, hierarchical fibers and semi-interpenetrating structured hydrogel can significantly improve surface areas.[7-12] Considering the porous structure as well as the large amount of various active

adsorption sites, three-dimensional graphene aerogel is a promising adsorbent for uranium extraction.[13-15] For example, an ethylenediamine cross-linked graphene aerogel exhibited a maximum adsorption capacity of 238.7 mg/g at pH 4.0.[16] By introduction of fungus hypha skeletons, abundant oxygen and nitrogen containing groups were introduced in the graphene aerogel structure. The resultant fungus hypha/graphene aerogel achieved an adsorption capacity of 288.6 mg/g at pH 5.0.[17] The open and porous structure of graphene aerogel is also important to facilitate rapid mass transport.[18]

The adsorption ability of an adsorbent is also determined by the traits and availability of its favorable adsorption sites. The nitrogen-based ligand, especially amidoxime, is the most efficient chelating group owing to its high affinity towards uranyl species in seawater.[9-11, 19, 20] The poly(amidoxime) hydrogel owned a uranium uptake capacity of 4.9 mg/g in natural seawater within four weeks.[11] The amidoxime-based polymeric fibers exhibited even higher adsorption capacity, which reached 11.5 mg/g in natural seawater after 90 days. Combing amidoxime with other functional groups like amino and carboxyl can further improve the adsorption capacity and selectivity. It is imperative to develop novel functional ligands in coordination with amidoxime group to enhance selectivity and capacity simultaneously.[7, 21-24] Among the variety candidates, β-cyclodextrin (βCD) derivatives have demonstrated great potentials for uranium extraction according to the host-guest interaction and complexation effect.[25-27] Particularly, carboxymethyl-β-cyclodextrin (CMCD) displays attractive uranium

enrichment characteristics attributing to its rich oxygen-containing functional groups.[24] Besides, CMCD also favors to form graphene aerogel with improved mechanical strength.[27]

In our previous work, we prepared succinyl-β-cyclodextrin-based membranes to extract uranium by grafting succinyl-β-cyclodextrin onto a polyacrylonitrile membrane. Here, we envisioned that a high-performance sorbent for oceanic uranium extraction can be prepared by integrating the advantageous qualities of graphene aerogel in capacity and kinetics with that of amidoxime groups and βCD derivatives in affinity and selectivity. On the one hand, graphene aerogel with larger surface area provided more active sites than membranes. On the other hand, CMCD served as an alternative to succinyl-β-cyclodextrin, given that CMCD is more readily available. Furthermore, amidoxime groups were introduced in the aerogel to further enhance the selectivity and uranium adsorption capacity. Motivated by these merits, the amidoxime functionalized diaminomaleonitrile (DMAO) and CMCD modified graphene oxide aerogel (GDC) was obtained via a one-step hydrothermal method. The morphology, structure, and adsorption behaviors of the GDC in both laboratory conditions and natural seawater were systematically investigated. Moreover, the uranium extraction was explored by applying an adsorbent module with the existence of oil contamination. Density functional theory (DFT) calculations were also performed to reveal the interaction between UO_2 and GDC. The significant adsorption performance coupled with the facile

preparation demonstrates the promising potential of using GDC for efficient and selective oceanic uranyl extraction.

RESULTS AND DISCUSSION

Preparation and characterization of GDC. GDC was prepared by a facile hydrothermal method. Briefly, the homogeneous solution containing a desired amount of GO, DMAO and CMCD was sealed in a Teflon-lined autoclave and heated at 120°C for 10 h to form hydrogel. Then, the hydrogel was dialyzed and freeze-dried to obtain GDC. In addition, three-dimensional self-assembled graphene aerogel (GA), DMAO cross-linked graphene aerogel (GD) and β-cyclodextrin/graphene composites (GC) were also prepared as references. The synthetic routes were shown in Figure 1. The preparation details and optimization experiments were described in the Supplementary Data.

Surface morphologies of three kinds of aerogels were characterized by SEM. The aerogels exhibited typical three-dimensional porous structure (Figure 1 and Figure S3). Compared with GA, GD possessed more pores due to the cross-linking of DMAO on GO sheets. Noteworthily, CMCD might further increase the interlayer spacing of GO sheets and avoid overlapping by π-π stacking interactions, leading to more pores in GDC than those in GD.

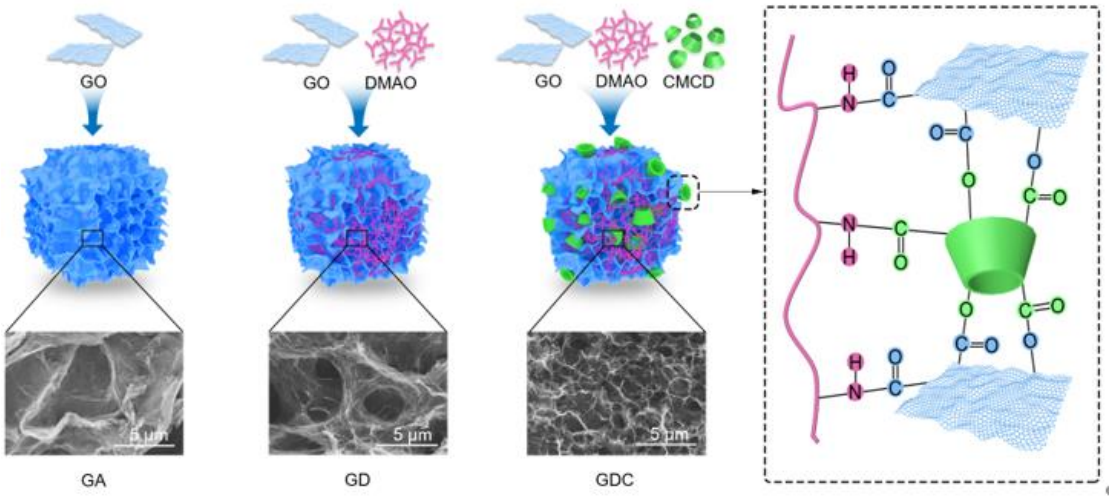

Figure 1. One-pot hydrothermal synthesis and SEM images of GA, GD and GDC. Possible mechanism of GDC synthesis.

XPS spectra of the aerogels were recorded to analyze the elemental compositions of GDC as well as grafting ratios of DMAO and CMCD (Figure 2a-c). In Figure 2a, the N1s peaks of GDC were deconvoluted in three peaks at 399.1 eV, 400.0 eV and 400.7 eV, which were assigned to HO-N=C-, -NH- and -NH_2, resulting from the introduction of DMAO.[3] According to Table S1, -NH- was the predominant form for N element in GD and GDC, indicating that -NH_2 in DMAO reacted with oxygen-containing groups. Moreover, the ratio of -NH- in GDC was higher than that in GD, which confirmed the reaction between CMCD and DMAO. Similar conclusions could be obtained from C 1s spectra of aerogels. As shown in Figure 2b and 2c, the C 1s high resolution spectra of GDC and GD were curve-fitted by four peaks (284.8 eV, 285.7 eV, 286.3 eV, 287.8 eV) correspond to C-C/C=C, C-N/C=N, C-O and C=O, respectively.[30] The peak appeared at 285.7 eV demonstrated the successful cross-linking of DMAO on GD and

131 GDC. In addition, GDC possessed more C-O and C=O than GD due to the abundant
132 oxygen-containing groups in CMCD. According to the relative ratios of elements
133 determined from XPS (Table S2), the roughly estimated grafting ratios of DMAO and
134 CMCD in GDC were calculated to be 14.1% and 85.3%.

135 FT-IR spectroscopy was used to verify the effective synthesis of prepared samples
136 (Figure 2d). Typical peaks of GO were found in the spectra of GA. The band at 1110
137 cm^{-1} was assigned to the C-O-C stretching vibration and the benzene ring frame
138 vibration was detected at 1402 and 1577 cm^{-1}, respectively.[31] The C=O stretching
139 vibration of -COOH and the O-H stretching vibration located at 1726 and 3435 cm^{-1}.[32]
140 For GD, the feature at 942 cm^{-1} was observed due to the C-N, C=N, N-O and O-H
141 groups, implying the successful preparation of GD.[33] The FT-IR spectrum of GDC
142 exhibited similar peaks to GD, while the stretching vibration located at 3432 cm^{-1}
143 became more obvious, which was caused by the abundant -OH groups of CMCD.

144 The XRD patterns are presented in Figure 2e and Table S3. GO showed a diffraction
145 peak at around 10° with an interlayer spacing (d-spacing) of 1.139 nm.[34] While GA,
146 GD and GDC presented broad diffraction peaks at around 25°, suggesting most of the
147 oxygen-containing groups of GO were reduced during the hydrothermal process.[35] The
148 d-spacings of GA, GD and GDC were 0.3356, 0.3437 and 0.3605 nm, respectively.
149 This result revealed that DMAO and CMCD could enhance the distance between the
150 graphene layers and improve porosity of aerogels. Among the three aerogels, GDC had
151 the largest BET surface area and highest porosity (Table S4), which demonstrated that

crosslinking of DMAO and addition of CMCD favored the formation of pore structures and provided more adsorption active sites.[36]

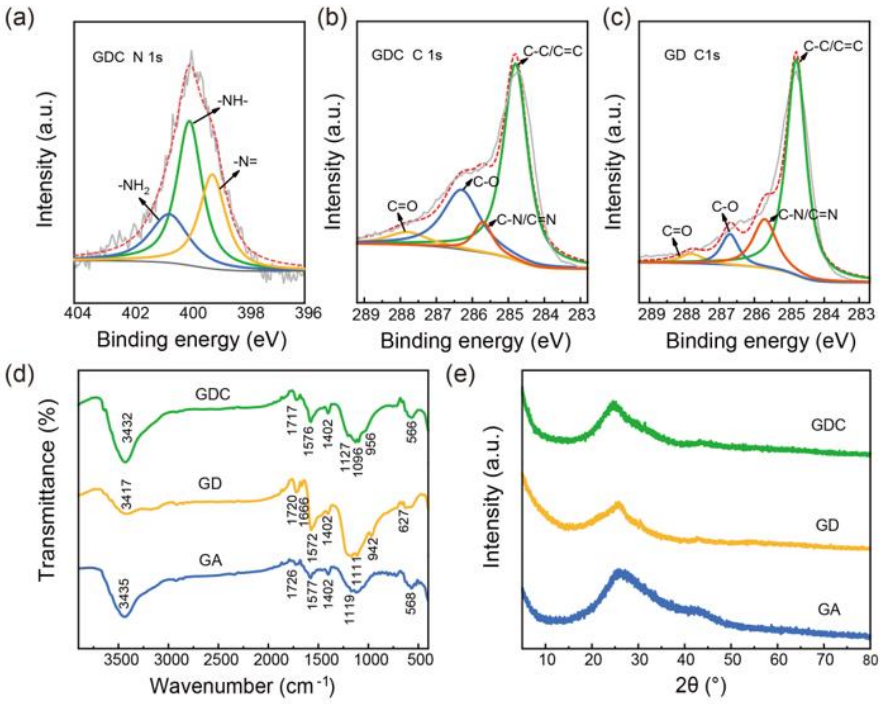

Figure 2. XPS spectra of (a) N 1s and (b) C 1s for GDC. (c) XPS spectra of C 1s for GD. (d) FT-IR spectra of GA, GD and GDC. (e) XRD patterns of GA, GD and GDC.

GDC for uranium adsorption and recovery. The initial pH of uranyl solutions plays a crucial role on the adsorption behavior by affecting the surface charge of the adsorbent and U(VI) speciation.[37] Figure 3a shows that three aerogels are all negatively charged at pH > 4.0. The adsorption capacities of GDC at different pH are shown in Figure 3b. The U(VI) uptake of GDC achieved the maximum value (642.8 mg/g) at pH 6.0, and the adsorption capacity decreased when the pH moved away from this optimum pH value. When pH < 6.0, uranium is predominantly present as positively charged species ($(UO_2(OH)^+$, $(UO_2)_3(OH)_5^+$, $(UO_2)_2(OH)_2^{2+}$, etc.).[38] The surface of GDC became less

negatively charged at lower pH, it even became positively charged at pH = 2.0. This reduced the electrostatic attraction between GDC and the positively charged uranium species, leading to lower adsorption capacity. At pH > 6.0, $(UO_2)_3(OH)_7^-$ and the $UO_2(OH)_2$ precipitate gradually increased at higher pH, causing the decrease in the adsorption capacity of U(VI).[38]

A series of adsorption experiments with different reaction times were performed to describe the U(VI) uptake rate (Figure 3c). The U(VI) adsorption of three adsorbents were extremely rapid at the beginning and gradually approached equilibrium. The increased adsorption capacity and shortened equilibrium time of GD relative to GA implied the great uranium affinity of DMAO. Noteworthily, GDC exhibited the highest adsorption rate and uranium uptake, which was possibly due to metal complexation from hydroxyl groups inside CMCD cavity.[28] In addition, the adsorption capacity of GDC for uranium (642.3 mg/g) is larger than the total uranium uptakes on GD (421.4 mg/g) and GC (213.6 mg/g), revealing that there is a synergistic effect between DMAO and CMCD for uranium adsorption. As exhibited in Figure 3d and Table S5, the adsorption process could be better described by the pseudo-second-order model. The equilibrium capacities calculated by the pseudo-second-order model were 628.9, 657.9, and 675.7 mg/g for 50, 100, and 200 mg/L U(VI) initial concentrations, respectively. These calculated data corresponded well with the experimental capacities, which confirmed that complexes with U(VI) were formed on the surface of GDC and the adsorption process is a chemisorption.[39]

The adsorption isotherms of GDC were also investigated (Figure 3e, Figure S7 and Table S6). The U(VI) uptake increased with the increase of initial uranium concentration, which was consistent with the observation from adsorption kinetics. Langmuir model fitted the equilibrium adsorption data better than the other two models at different temperatures, which demonstrated that the dominant adsorption process was a monolayer adsorption.[40] According to Langmuir model, the maximum U(VI) adsorption capacity was calculated to be 654.2 mg/g at 25°C. The adsorption performance of GDC and some relevant adsorbents was summarized in Table S7. GDC exhibited higher adsorption capacity and shorter equilibrium time than the reported adsorbents.

Besides adsorption capacity and equilibrium time, reusability of adsorbents is another challenge in uranium extraction, since it greatly affects the operation cost. Consecutive adsorption-desorption cycles were performed to evaluate the reusability of GDC.[41] The GDC maintained a high reusability of 87.3% and kept integrality after ten regeneration cycles indicating the great reusability and stability of GDC.

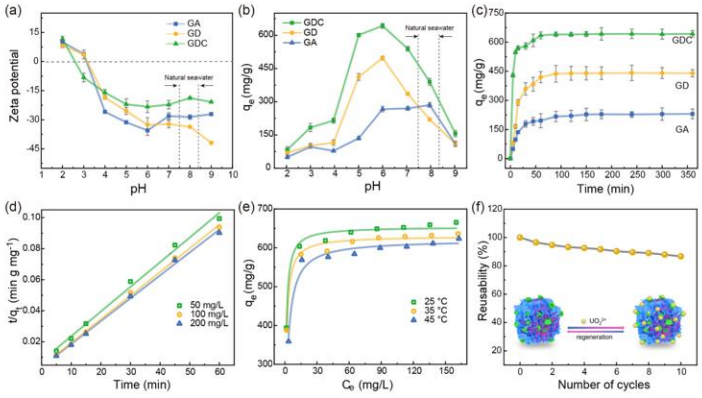

Figure 3. (a) Zeta potential of GA, GD and GDC as a function of pH. (b) Influence of pH on U(VI) adsorption efficiency with the same adsorption time of 24 h. (c) Effect of adsorption time for GA, GD and GDC at pH = 6.0. (d) Pseudo-second-order kinetic model fit for the U(VI) adsorption of GDC with the initial U(VI) concentrations of 50, 100 and 200 mg/L. (e) Langmuir isotherms for U(VI) adsorption of GDC at 25°C, 35°C and 45°C (pH = 6.0). (f) Reusability of GDC in ten adsorption–desorption cycles.

Uranium dynamic adsorption was conducted using a GDC block (0.0273 g) as the filter to treat a uranium solution continuously. The video of dynamic adsorption process was shown in supplemental data and the removal efficiency achieved nearly 100%. Encouraged by the result, a series of adsorbent modules with different lengths were designed to promote the treatment capacity and demonstrate realistic application of GDC. The removal efficiency increased from 98.7% to 100% with the increase of the module length from 2 to 5 cm (Figure 4a and Table S8). This phenomenon suggested potential advantageous of GDC modules for uranium adsorption, such as flexible size and multiple connection modes.

Selectivity of GDC for uranium. Oil fouling shortens the lifetime of the adsorbents and increases the total cost of uranium extraction. Therefore, oil resistance makes significant contribution towards the long-term use of adsorbents. The hydrophilic property of aerogels was evaluated by water contact angle. The GA showed a water contact angle of 59.3° (Figure S5). The GD and GDC exhibited ultra-low water contact angles (0°), because the water drops spread out once they touched to the aerogel

surfaces (Figure 4d and Figure S5). The low contact angle indicated the excellent hydrophilicity of GD and GDC. Furthermore, the underwater oil contact angle of GDC was also identified to be 106°. The -COOH and -NH_2 on DMAO and -OH on CMCD contributed to the great hydrophilicity.[42] To gain more insight on oil resistance, adsorption experiments in uranium solution containing oil drops were performed. Mineral oil and dichloromethane were added to the uranium solutions with the oil volume ratios ranged from 20% to 80%. The GDC was then immerged into the as-formed emulsion slowly. The U(VI) removal efficiency kept at nearly 100% after 2 h operation, which suggests good oil resistance of GDC. In the dynamic process, 50 mL of oil and 250 mL of U(VI) solution (100 mg/L) were mixed and the mixture was pumped through a 5 cm GDC module. The filtrate was collected and the GDC module was back flushed by deionized water. The filtration/back flushing processes were repeated for ten times. As exhibited in Figure S8, the removal efficiency of U(VI) decreased slightly with increasing the filtration cycles, which indicated the excellent oil resistance of GDC.

Given the abundance of competing ions in natural seawater, selectivity is considered as a vital factor that greatly influences adsorbents in the practical applications. The solution containing uranium and six other metal ions with the concentration of 10 mg/L was used to assess the effects of metal ions. Figure 4b shows the uptake of Ca, Co, Cu, Fe, Mg, V and U by GDC, the adsorbent achieved a higher capacity (32.8 mg/g) for U than other elements in 24 h, displaying the great selectivity of GDC. This can be

244 explained by the strong uranium ion anchoring via amidoxime and the internal cavity
245 of CMCD. Besides, GDC also presented good selectivity when the anions existed
246 (Figure 4c). Cl^-, NO_3^- and SO_4^{2-} almost had no impact on uranium removal. Although
247 HCO_3^-, CO_3^{2-} and PO_4^{3-} reduced the removal efficiency of uranium, their concentrations
248 far exceed their actual contents in natural seawater.[9] Electrostatic repulsion occurred
249 between GDC and these anions, which is partially responsible for the negligible impact
250 of anions.

251 U(VI) adsorption ability of GDC in natural seawater was also studied. The removal
252 efficiencies and adsorption rates of the competitive ions, including Fe^{3+}, Co^{2+}, Zn^{2+},
253 Mg^{2+}, Ca^{2+}, VO_4^{3-}, Ni^{2+}, and Pb^{2+}, were lower than those of uranyl, which proved that
254 GDC is a promising adsorbent for uranium capture from seawater. The uranium uptake
255 reached 19.7 mg/g after 21 days when the GDC was exposed in 50 L of natural seawater
256 (Figure 4e). The uranium extraction efficiency in natural seawater of GDC is much
257 higher than the previously reported adsorbents (Figure 4f and Table S9),[10, 43-47]
258 implying great promise of high-performance amidoxime and βCD decorated graphene
259 aerogel adsorbent for uranium recovery from natural seawater and nuclear waste.

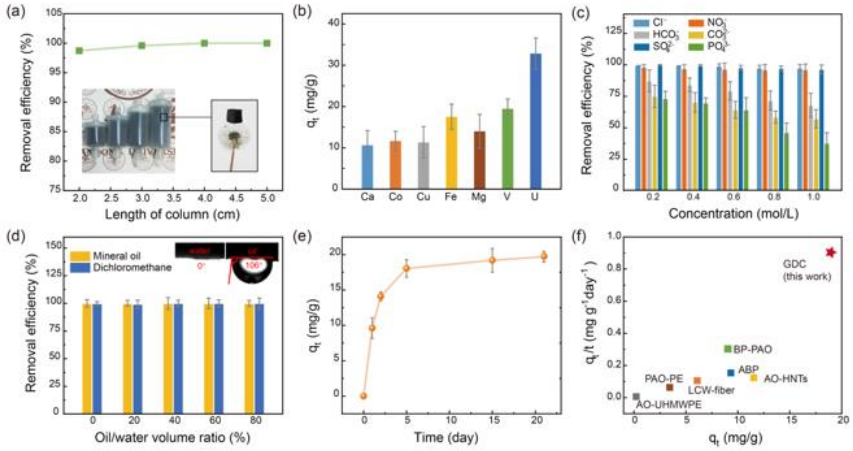

Figure 4. (a) Adsorption capacities of different columns. Insets are photos of GDC modules and GDC. (b) Adsorption capacities of GDC for various metal ions (metal ions initial concentration = 10 mg/L, adsorption time = 24 h). (c) Effect of different anions ($C_{(U(VI))}$ = 50 mg/L, $V_{(U(VI))}$ = 200 mL, m_{GDC} = 30 mg). (d) Effect of oils with different concentrations on removal efficiency of U(VI) in 100 mg/L uranium solution. (e) U(VI) adsorption capacity of GDC in natural seawater for 21 days. (f) Comparison with other adsorbents reported in previously reported works.[10, 43-47]

Adsorption mechanisms. FTIR and XPS analysis were used to investigate the uranium adsorption mechanisms. Figure 5a shows the FTIR spectra of the U(VI) adsorbed GDC (GDC-U) and U(VI) desorbed GDC. A new peak at 926 cm^{-1} appeared due to the asymmetric vibration of O=U=O for GDC-U, implying the immobilization of U(VI). While in the spectrum of desorbed GDC, this peak disappeared due to the nearly complete desorption of U(VI). Similar phenomenon was also observed in the XPS spectra (Figure 5b). It was worth to note that the peak of O 1s in the high resolution XPS spectra of GDC-U (Figure 5e) was de-convoluted into three components,

corresponding to O-C (533.7 eV), O-H (532.8 eV) and O=C (531.8 eV), respectively. Compared with GDC, the peak area of -OH of GDC-U decreased from 30.7% to 20.2%, the atomic percent value of O in GDC-U deduced from 43.2% to 20.1%. Meanwhile, the relative -NH_2 peak area value of GDC-U decreased to 22.3% (Table S1). These results indicated the U(VI) adsorption on GDC surface is related to O-containing and N-containing functional groups. As described in Figure 5g, the coordination and chelation effect of amidoxime, amine, hydroxyl, and other O-containing groups contributed to improving the uranium adsorption capacity of GDC. According to DFT calculations in our prior research, UO_2^{2+} exhibits a strong interaction with βCD.[48] In this work, DFT calculations were conducted to explore the interaction between UO_2^{2+} and DMAO. To obtain the reasonable structure of the DMAO- UO_2^{2+} complex, various starting geometries and explored different hydration systems were considered. As shown in Figure S12, UO_2^{2+} is tend to bind with oxime type N and O, which is consistent with the calculations of Liu et al.[49] The binding energy of the most stable hydration complexes $[UO_2\text{-DMAO-3}(H_2O)]^{2+}$ is -44.2 Kcal/mol. The strong interaction of UO_2-βCD, UO_2-DMAO and the abundant active sites in graphene aerogel resulted in the improved uranium adsorption capacity of GDC. Moreover, the binding free energy between $[UO_2(H_2O)_4]^{2+}$ and βCD is larger than those for the other hydrated metal ions, indicating good selectivity of βCD with U(VI). [48] The excellent selectivity of amidoxime for U(VI) can also be evidenced by the higher binding free energy between amidoxime and UO_2^{2+} than those for other metal ions (Sr^{2+}, Cs^{+}, Fe^{3+}, etc.).

Accordingly, the obtained GDC favored the adsorption of U(VI) over other ions, owing to the strong interactions of UO_2^{2+}-βCD and UO_2^{2+}-amidoxime.

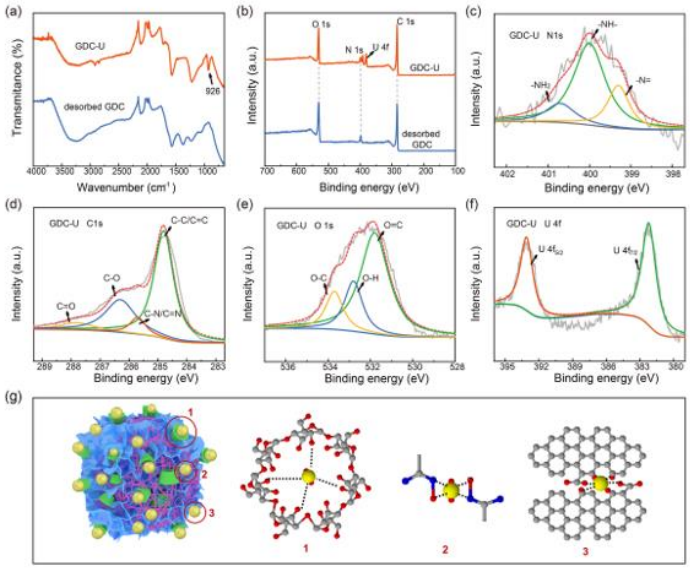

Figure 5. (a) FTIR spectra of GDC-U and U(VI) desorbed GDC. (b) XPS spectra of GDC-U and U(VI) desorbed GDC. XPS spectra of (c) N 1s, (d) C 1s, (e) O 1s and (f) U 4f for GDC-U. (g) Adsorption mechanisms of GDC.

ENVIRONMENTAL IMPLICATIONS

In summary, a superhydrophilic and oil resistance aerogel adsorbent with great U(VI) adsorption performance was constructed by a facile one-pot hydrothermal synthesis. The three-dimensional graphene macrostructure and cavity of CMCD endows GDC with high specific surface area and adsorption active sites. The introduction of amidoxime group further improves the uranium adsorption capacity as well as the selectivity of GDC. Even after ten regeneration cycles, GDC still showed the reusability

of 87.3%. In the long-term adsorption in natural seawater, GDC achieved the uptake of 19.7 mg/g for 21 days, which is higher than most reported works. Highly efficient adsorption of U(VI) on GDC was also achieved in a dynamic test, which further confirmed the hydrophily and practicability of GDC. The mechanism of U(VI) adsorption was symmetrically studied and the uranium adsorption could be attributed to the coordination or chelation of amidoxime, amine, hydroxyl and other O-containing groups. The results demonstrate GDC as a potential adsorbent for rapid, efficient, selective and anti-oil pollution extraction of uranium from uranium-containing water.

ASSOCIATED CONTENT

Supporting Information. Additional text with experimental details, DFT computational details, optimization conditions, adsorption isotherms and kinetics, GDC modules. 18 figures showing preparation scheme procedures, adsorption optimization conditions, SEM images, XPS spectra, contact angle photos, adsorption kinetics and isotherms, GDC modules and their adsorption performance, DFT optimized structures and comparison with other adsorbents; eleven tables listing parameters of XPS, XRD, BET, adsorption isotherm, kinetics and modules. DFT computational results and comparation with other adsorbents (PDF). The videos of compressions, oil-water separation and dynamic adsorption process (MP4)

AUTHOR INFORMATION

Corresponding Author

*Phone: +86-53258630929; e-mail: wangzhn@sdu.edu.cn

Notes

The authors declare no competing financial interest.

ACKNOWLEDGMENT

This work was supported by the National Natural Science Foundation of China (22078175 and 21878177), the Natural Science Foundation of Shandong Province (ZR2019LFG003).

338 REFERENCES

339 (1) Burns, P. C.; Ewing, R. C.; Navrotsky, A. Nuclear fuel in a reactor accident.
340 *Science* **2012**, *335*, 1184-1188.
341 (2) Wu, F.; Pu, N.; Ye, G.; Sun, T.; Wang, Z.; Song, Y.; Wang, W.; Huo, X.; Lu, Y.;
342 Chen, J. Performance and mechanism of uranium adsorption from seawater to
343 poly(dopamine)-inspired sorbents. *Environ. Sci. Technol.* **2017**, *51*, 4606-4614.
344 (3) Sholl, D. S.; Lively, R. P. Seven chemical separations to change the world, *Nature*
345 **2016**, *532*, 435-437.
346 (4) Ju, P.; Liu, Q.; Zhang, H.; Chen, R.; Liu, J.; Yu, J.; Liu, P.; Zhang, M.; Wang, J.
347 Hyperbranched topological swollen-layer constructs of multi-active sites
348 polyacrylonitrile (PAN) adsorbent for uranium(VI) extraction from seawater. *Chem.*
349 *Eng. J.* **2019**, *374*, 1204-1213.
350 (5) Abney, C. W.; Mayes, R. T.; Saito, T.; Dai, S. Materials for the recovery of
351 uranium from seawater. *Chem. Rev.* **2017**, *117*, 13935-14013.
352 (6) Xie, Y.; Chen, C.; Ren, X.; Wang, X.; Wang, H.; Wang, X. Emerging natural and
353 tailored materials for uranium-contaminated water treatment and environmental
354 remediation. *Prog. Mater. Sci.* **2019**, *103*, 180-234.
355 (7) Luo, W.; Xiao, G.; Tian, F.; Richardson, J. J.; Wang, Y.; Zhou, J.; Guo, J.; Liao,
356 X.; Shi, B. Engineering robust metal-phenolic network membranes for uranium
357 extraction from seawater. *Energy Environ. Sci.* **2019**, *12*, 607-614.

(8) Wang, C.; Zheng, T.; Luo, R.; Liu, C.; Zhang, M.; Li, J.; Sun, X.; Shen, J.; Han, W.; Wang, L. In situ growth of ZIF-8 on PAN fibrous filters for highly efficient U(VI) removal. *ACS Appl. Mater. Interfaces* **2018**, *10*, 24164-24171.

(9) Xu, X.; Zhang, H.; Ao, J.; Xu, L.; Liu, X.; Guo, X.; Li, J.; Zhang, L.; Li, Q.; Zhao, X.; Ye, B.; Wang, D.; Shen, F.; Ma, H. 3D hierarchical porous amidoxime fibers speed up uranium extraction from seawater. *Energy Environ. Sci.* **2019**, *12*, 1979-1988.

(10) Wu, G.; Liu, Y.; Zheng, Q.; Yu, Z.; Luo, F. Ultrahigh uranium extraction performance of COFs/SPES mixed matrix membranes at acidic medium. *J. Solid State Chem.* **2020**, *288*, 121364.

(11) Ma, C.; Gao, J.; Wang, D.; Yuan, Y.; Wen, J.; Yan, B.; Zhao, S.; Zhao, X.; Sun, Y.; Wang, X.; Wang, N. Sunlight polymerization of poly(amidoxime) hydrogel membrane for enhanced uranium extraction from seawater. *Adv. Sci.* **2019**, *6*, 1900085.

(12) Zhao, D.; Wang, Y.; Zhao, S.; Wakeel, M.; Wang, Z.; Shaikh, R. S.; Hayat, T.; Chen, C. A simple method for preparing ultra-light graphene aerogel for rapid removal of U(VI) from aqueous solution. *Environ. Pollut.* **2019**, *251*, 547-554.

(13) Worsley, M. A.; Pham, T. T.; Yan, A.; Shin, S. J.; Lee, J. R. I.; Hansen, M.; Mickelson, W.; Zettl, A. Synthesis and characterization of highly crystalline graphene aerogels, *ACS Nano* **2014**, *8*, 11013-11022.

(14) Worsley, M. A.; Pauzauskie, P. J.; Olson, T.Y.; Biener, J.; Satcher, J. H.; Jr; Baumann, T. F. Synthesis of graphene aerogel with high electrical conductivity, *J. Am. Chem. Soc.* **2010**, *132*, 14067–14069.

(15) Zhu, C.; Liu, T.; Qian, F.; Han, Y. J.; Duoss, E. B.; Kuntz, J. D.; Spadaccini, C. M.; Worsley, M. A.; Li, Y. Supercapacitors based on three-dimensional hierarchical graphene aerogels with periodic macropores, *Nano Lett.* **2016**, *16*, 3448–3456.

(16) Li, Y.; Li, L.; Chen, T.; Duan, T.; Yao, W.; Zheng, K.; Dai, L.; Zhu, W. Bioassembly of fungal hypha/graphene oxide aerogel as high performance adsorbents for U(VI) removal. *Chem. Eng. J.* **2018**, *347*, 407-414.

(17) Zhu, C.; Han, T. Y.; Duoss, E. B.; Golobic, A. M.; Kuntz, J. D.; Spadaccini, C. M.; Worsley, M. A. Highly compressible 3D periodic graphene aerogel microlattices. *Nat. Commun.* **2015**, *6*, 8.

(18) Ofili, N. E. R.; Thetford, A.; Kaltsoyannis, N. Adsorption of U(VI) on stoichiometric and oxidised mackinawite: a DFT Study. *Environ. Sci. Technol.* **2020**, *54*, 6792-6799.

(19) Sun, Q.; Aguila, B.; Earl, L. D.; Abney, C. W.; Wojtas, L.; Thallapally, P. K.; Ma, S. Covalent organic frameworks as a decorating platform for utilization and affinity enhancement of chelating sites for radionuclide sequestration. *Adv. Mater.* **2018**, *30*, 1705479.

(20) Yuan, Y.; Feng, S.; Feng, L.; Yu, Q.; Liu, T.; Wang, N. A bio-inspired nano-pocket spatial structure for targeting uranyl capture. *Angew. Chem. Int. Ed.* **2020**, *59*, 4262-4268.

(21) Xu, L.; Zhang, D.; Ma, F.; Zhang, J.; Khayambashi, A.; Cai, Y.; Chen, L.; Xiao, C.; Wang, S. Nano-MOF^{+} technique for efficient uranyl remediation. *ACS Appl. Mater. Interfaces* **2019**, *11*, 21619-21626.

(22) Kou, S.; Yang, Z.; Sun, F. Protein hydrogel microbeads for selective uranium mining from seawater. *ACS Appl. Mater. Interfaces* **2017**, *9*, 2035-2039.

(23) Yu, Q.; Yuan, Y.; Feng, L.; Feng, T.; Sun, W.; Wang, N. Spidroin-inspired, high-strength, loofah-shaped protein fiber for capturing uranium from seawater. *Angew. Chem. Int. Ed.* **2020**, *59*, 15997-16001.

(24) Helal, A. S.; Mazario, E.; Mayoral, A.; Decorse, P.; Losno, R.; Lion, C.; Ammar, S.; Hemadi, M. Highly efficient and selective extraction of uranium from aqueous solution using a magnetic device: succinyl-beta-cyclodextrin-APTES@maghemite nanoparticles. *Environ. Sci. Nano* **2018**, *5*, 158-168.

(25) Li, H.; Zhou, F.; He, B.; Wang, G.; Xie, W.; Liang, E. Efficient adsorption of heavy metal ions by a novel AO-PAN-g-chitosan/Fe_3O_4 composite. *Chemistryselect* **2020**, *5*, 8033-8039.

(26) Alsbaiee, A.; Smith, B. J.; Xiao, L.; Ling, Y.; Helbling, D. E.; Dichtel, W. R. Rapid removal of organic micropollutants from water by a porous β-cyclodextrin polymer. *Nature* **2016**, *529*, 190-194.

(27) Chalasani, R.; Vasudevan, S. Cyclodextrin-functionalized Fe_3O_4@TiO_2: Reusable, magnetic nanoparticles for photocatalytic degradation of endocrine-disrupting chemicals in water supplies. *ACS Nano* **2013**, *7*, 4093-4104.

(28) Sun, Z.; Zhao, L.; Liu, C.; Zhen, Y.; Zhang, W.; Ma, J. A novel 3D adsorbent of reduced graphene oxide-β-cyclodextrin aerogel coupled hardness with softness for efficient removal of bisphenol A. *Chem. Eng. J.* **2019**, *372*, 896-904.

(29) Qiu, Y.; Shi, Q.; Zhou, L.; Chen, M.; Chen, C.; Tang, P.; Walker, G. S.; Wang, P. NiPt nanoparticles anchored onto hierarchical nanoporous N-doped carbon as an efficient catalyst for hydrogen generation from hydrazine monohydrate. *ACS Appl. Mater. Interfaces* **2020**, *12*, 18617-18624.

(30) Bai, J.; Chu, J.; Yin, X.; Wang, J.; Tian, W.; Huang, Q.; Jia, Z.; Wu, X.; Guo, H.; Qin, Z. Synthesis of amidoximated polyacrylonitrile nanoparticle/graphene composite hydrogel for selective uranium sorption from saline lake brine. *Chem. Eng. J.* **2020**, *391*, 123553.

(31) Mu, B.; Li, M. Fabrication and thermal properties of tetradecanol/graphene aerogel form-stable composite phase change materials. *Sci. Rep.* **2018**, *8*, 8878.

(32) Yang, P.; Zhang, H.; Liu, Q.; Liu, J.; Chen, R.; Yu, J.; Hou, J.; Bai, X.; Wang, J. Nano-sized architectural design of multi-activity graphene oxide (GO) by chemical post-decoration for efficient uranium(VI) extraction. *J. Hazard. Mater.* **2019**, *375*, 320-329.

(33) Li, R.; Chen, C.; Li, J.; Xu, L.; Xiao, G.; Yan, D. A facile approach to superhydrophobic and superoleophilic graphene/polymer aerogels. *J. Mater. Chem. A* **2014**, *2*, 3057-3064.

(34) Xu, L.; Xiao, G.; Chen, C.; Li, R.; Mai, Y.; Sun, G.; Yan, D. Superhydrophobic and superoleophilic graphene aerogel prepared by facile chemical reduction. *J. Mater. Chem. A* **2015**, *3*, 7498-7504.

(35) Xin, S.; Liu, G.; Ma, X.; Gong, J.; Ma, B.; Yan, Q.; Chen, Q.; Ma, D.; Zhang, G.; Gao, M.; Xin, Y. High efficiency heterogeneous Fenton-like catalyst biochar modified $CuFeO_2$ for the degradation of tetracycline: Economical synthesis, catalytic performance and mechanism. *Appl. Catal. B* **2021**, *280*, 119386.

(36) Liang, H.; Cao, X.; Zhang, W.; Lin, H.; Zhou, F.; Chen, L.; Yu, S. Robust and highly efficient free-standing carbonaceous nanofiber membranes for water purification. *Adv. Funct. Mater.* **2011**, *21*, 3851-3858.

(37) Xiao, J.; Xie, S.; Jing, Y.; Yao, Y.; Wang, X.; Jia, Y. Preparation of halloysite@graphene oxide composite and its application for high-efficient decontamination of U(VI) from aqueous solution. *J. Mol. Liq.* **2016**, *220*, 304-310.

(38) Tian, C.; Zhao, J.; Ou, X.; Wan, J.; Cai, Y.; Lin, Z.; Dang, Z.; Xing, B. Enhanced adsorption of p-arsanilic acid from water by amine-modified UiO-67 as examined using extended X-ray absorption fine structure, X-ray photoelectron spectroscopy, and density functional theory calculations. *Environ. Sci. Technol.* **2018**, *52*, 3466-3475.

(39) Bai, Z.; Liu, Q.; Zhang, H.; Yu, J.; Chen, R.; Liu, J.; Song, D.; Li, R.; Wang, J. Anti-biofouling and water-stable balanced charged metal organic framework-based polyelectrolyte hydrogels for extracting uranium from seawater. *ACS Appl. Mater. Interfaces* **2020**, *12*, 18012-18022.

(40) Zhang, Y.; Yan, K.; Ji, F.; Zhang, L. Enhanced removal of toxic heavy metals using swarming biohybrid adsorbents. *Adv. Funct. Mater.* **2018**, *28*, 1806340.

(41) Xiao, F.; Sun, Y.; Du, W.; Shi, W.; Wu, Y.; Liao, S.; Wu, Z.; Yu, R. Smart photonic crystal hydrogel material for uranyl ion monitoring and removal in water. *Adv. Funct. Mater.* **2017**, *27*, 1702147.

(42) Klimchuk, S.; Shang, M.; Samuel, M. S.; Niu, J. Robust hybrid hydrophilic coating on a high-density polyethylene surface with enhanced mechanical property. *ACS Appl. Mater. Interfaces* **2020**, *12*, 32017-32022.

(43) Zhao, S.; Yuan, Y.; Yu, Q.; Niu, B.; Liao, J.; Guo, Z.; Wang, N. A dual-surface amidoximated halloysite nanotube for high-efficiency economical uranium extraction from seawater. *Angew Chem. Int. Ed. Engl.* **2019**, *58*, 14979-14985.

(44) Hu, J.; Ma, H.; Xing, Z.; Liu, X.; Xu, L.; Li, R.; Lin, C.; Wang, M.; Li, J.; Wu, G. Preparation of amidoximated ultrahigh molecular weight polyethylene fiber by radiation grafting and uranium adsorption test. *Ind. Eng. Chem. Res.* **2015**, *55*, 4118-4124.

(45) Yuan, Y.; Niu, B.; Yu, Q.; Guo, X.; Guo, Z.; Wen, J.; Liu, T.; Zhang, H.; Wang, N. Photoinduced multiple effects to enhance eranium extraction from natural seawater by black phosphorus nanosheets. *Angew Chem. Int. Ed. Engl.* **2020**, *59*, 1220-1227.

(46) Pan, H.; Wai, C.; Kuo, L.; Gill, G. A.; Wang, J.; Joshi, R.; Janke, C. J. A highly efficient uranium grabber derived from acrylic fiber for extracting uranium from seawater. *Dalton Tran.* **2020**, *49*, 2803-2810.

(47) Kim, J.; Tsouris, C.; Oyola, Y.; Janke, C. J.; Mayes, R. T.; Dai, S.; Gill, G.; Kuo, L.; Wood, J.; Choe, K.; Schneider, E.; Lindner, H. Uptake of uranium from seawater by amidoxime-based polymeric adsorbent: Field experiments, modeling, and updated economic assessment. *Ind. Eng. Chem. Res.* **2014**, *53*, 6076-6083.

(48) Li, N.; Yang, L.; Ji, X.; Ren, J.; Gao, B.; Deng, W.; Wang, Z. Bioinspired succinyl-β-cyclodextrin membranes for enhanced uranium extraction and reclamation. *Environ. Sci. Nano* **2020**, *7*, 3124-3135.

(49) Liu, X.; Xie, S.; Wang, G.; Huang, X.; Duan, Y.; Liu, H. Fabrication of environmentally sensitive amidoxime hydrogel for extraction of uranium (VI) from an aqueous solution. *Colloids Surf. A Physicochem. Eng. Asp.* 2011, *611*, 125813

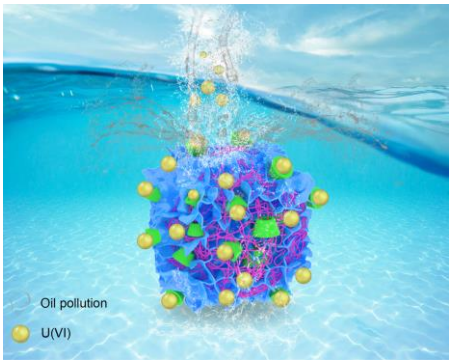

Table of Contents (TOC)

59 × 47 mm (300 × 300 DPI)